Pilot- and Industrial-Scale Experimental Investigation of Numerically Optimized Cyclones

Romualdo L. Salcedo*,† and Mário J. Pinho‡

Departamento de Engenharia Química, Faculdade de Engenharia da Universidade do Porto, Rua Dr. Roberto Frias s/n, 4200-465 Porto Codex, Portugal, and QUIMlGAL, Química de Portugal S.A., Quinta da Industria 3860 Estarreja, Portugal

A new geometry of reverse-flow gas cyclones obtained by numerical optimization was shown at the laboratory scale to be significantly more efficient than other high-efficiency designs. However, it is usually recognized that experimental results obtained with laboratory-scale or sampling cyclones cannot be extrapolated to pilot or industrial scales. The present paper confirms, at these larger scales, the significantly larger collection efficiencies obtained with the numerically optimized design compared to a competing high-efficiency design available on the marketplace for the capture of fine sulfanilic acid (median volume diameter of 17 μm) at a Portuguese chemical manufacturer. A partial recirculation system within a collector-first arrangement further reduces emissions without an appreciable increase in pressure drop. The experimentally verified efficiencies at the industrial scale varied between 99.58 and 99.64% for sulfanilic acid with pressure drops around 2.5 kPa. The numerically optimized cyclones, when coupled with a partial recirculation system, extend the applicability of these simple devices to the fine particle collection that is typical of more expensive devices, such as venturis and online pulse jet bag filters.

Introduction

Cyclones are gas−solid separation devices characterized by low investment and operating costs that can be used on heavily loaded gases or at high temperature and pressure. They are employed in many industries for two complementary purposes: air pollution control by reduction of atmospheric emissions to maximum admissible levels and raw material or product recovery. The development of cyclones with collection efficiencies significantly above those obtainable with currently available geometries, especially for particle diameters below 5 μm, could have a strong impact on the chemical process industries.[1] Many industries could then use these low investment and operating cost dedusters with the required efficiency to avoid having to resort to equipment or with much higher capital, operating, or maintenance costs, such as venturis and bag filters. Also, in some processes at high temperature (up to 1300 K) and pressure (up to 100 bar), cyclones are currently the only dedusters available.

In a typical reverse-flow cyclone (Figure 1), which is the most common type used, the dirty gas enters the cyclone tangentially at the top, describes a descending outer vortex, inverts the direction of motion, and ascends by an inner vortex exiting at the cyclone top through the vortex finder. The heavier (larger or denser) particles are swept to the cyclone wall by centrifugal forces that oppose a radial drag and are carried toward the cyclone bottom by the descending outer vortex. The finer particles exit at the top with the gas, together with coarser particles that might have been reentrained and swept by the ascending inner vortex. Reentrainment can occur as a result of an entry velocity that is excessive for the cyclone geometry and particle density.[2−4]

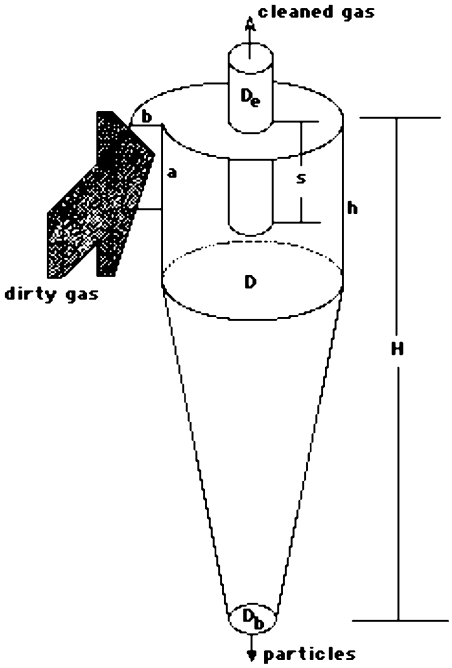

Figure 1. Reverse-flow cyclone.

The present work shows, at the pilot scale, the behavior of the numerically optimized RS_VHE cyclone design, extending previous work done at the laboratory scale.[5,6] It also shows, at both the pilot and industrial scales, the performance of the RS_VHE cyclone coupled with a partial recirculation system. A comparison is also made with the performance of a high-efficiency cyclone available on the marketplace and with an online pulse jet bag filter.

The results show that the proposed RS_VHE design typically reduces the emissions by 50% in comparison with the tested HE cyclone at comparable pressure drops, in agreement with the laboratory-scale data

* To whom all correspondence should be sent. Fax: +351225081440. E-mail: rsalcedo@fe.up.pt.
† Faculdade de Engenharia da Universidade do Porto
‡ QUIMlGAL.

10.1021/ie020195e CCC: $25.00
Published on Web 11/19/2002

comparing the RS_VHE and Stairmand HE designs.[6] The recirculation further reduces emissions by another 50%, putting this system at a level that is characteristic of high-performance venturis and online pulse jet bag filters.

Numerical Optimization of Reverse-flow Cyclones

The scientific literature is scarce on the subject of cyclone optimization most probably for two reasons: up to recently, no single theory could predict with reasonable accuracy the behavior of an arbitrary-geometry cyclone under different operating conditions,[5,7−10] and the possibility exists for commercial spin-offs derived from innovative geometries.[11] Also, it is highly unlikely that the optimum design can be found by empirical testing, as too many design parameters are involved. Thus, the problem of the optimization of reverse-flow cyclones has mostly been tackled on a trial-and-error basis.[1,12−14]

To our knowledge, only a few works are directly related to cyclone optimization based on a simulation model.[6,15−19] Dirgo and Leith[15] have used the Leith and Licht[20] collection model to predict cyclone performance. Pilot-scale tests with the optimized geometries, however, have failed to produce any significant improvements. Iozia and Leith[16] and Ramachandran and Leith[17] have used the logistic empirical collection efficiency model of Iozia and Leith[8] for simulation purposes. However, these authors have not performed a full optimization, as only five degrees of freedom (D_e, a, b, s, and H) were employed, whereas the other three cyclone design variables (D, h, and D_b) were held fixed.

In previous papers,[6,18] it was demonstrated that it is possible to design significantly improved reverse-flow cyclones by solving adequate numerical optimization problems. These equations concern the maximization of some profit function, viz., global efficiency, subject to the model equations (equality constraints) and inequality constraints (geometry, pressure drop, and saltation velocity). The Mothes and Löffler[7] theory was used as a modeling environment, coupled with an empirical estimate of the particles' turbulent dispersion coefficient.[5] This estimate predicts grade efficiency curves that agree reasonably well with the experimental data from various authors and is given by

$$Pe_p = 0.0342 Re_p^{1.263} \tag{1}$$

where $Pe_p = u_r d_p / D_r$ is the radial particle Peclet number, D_r is the radial dispersion coefficient, and $Re_p = \rho d_p u_r / \mu$ is the radial particle Reynolds number. The optimization was performed using a stochastic adaptive random search global optimizer.[21]

Ravi et al.[19] also followed a similar approach, using multiobjective optimization and genetic algorithms but considering a constant value for the particles' turbulent dispersion coefficient.

The main result of the numerical optimization was the geometry RS_VHE, which is significantly different from other high-efficiency geometries available in the literature,[6] including the optimum cyclone designs obtained by Iozia and Leith[16] and by Ravi et al.[19] This geometry is detailed in European patent application EP099670006, and its superior behavior at the laboratory scale, in comparison with a Stairmand HE design for the capture of fine $Ca(OH)_2$ can be found elsewhere.[6]

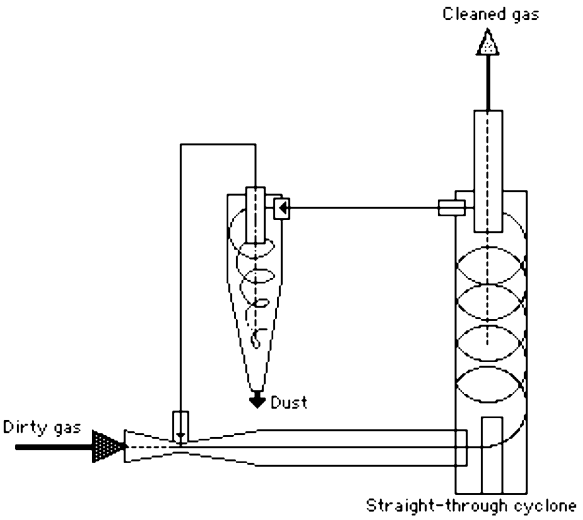

Figure 2. Concentrator-first recirculation system.

For example, a reduction in emissions of 53% was achieved on average, and the Moore and MacFarland[22,23] dimensionless performance index of the RS_VHE design, as compared with that from five different designs,[14] showed lower (better) values.

Recirculation Systems

One of the methods of increasing the collection efficiency of cyclone dedusters is to promote some recirculation of the exhaust gases. Recirculation systems composed of a dust concentrator, which can be a uniflow or straight-through cyclone (concentrator), coupled to a reverse-flow cyclone (collector) are described in the literature.[2,24,25] These systems, similar to that shown in Figure 2, can, under some circunstances, show collection efficiencies well above those of reverse-flow cyclones. Their collection efficiency is given by

$$\eta = \frac{\eta_c \eta_s}{1 - \eta_s + \eta_c \eta_s} \tag{2}$$

where η_c and η_s are, respectively, the cyclone (collector) and concentrator efficiencies, both computed within the loop. Thus, these systems are more efficient than single cyclones ($\eta > \eta_c$) of comparable geometry and size whenever $\eta_s > 1/(2 - \eta_c)$, viz., the concentrator must have a collection efficiency larger than that of the collector, both measured within the loop. An efficient system with a concentrator-first arrangement is described in European patent EP0430647.

However, it is possible to alter the system configuration to a collector-first sequence (Figure 3), where the system will always have a collection efficiency above that of the single reverse-flow cyclone operating within the loop.[3] A system composed of a reverse-flow collector followed by a straight-through concentrator is described in detail in International patent application WO0141934, with an efficiency given by

$$\eta = \frac{\eta_c}{1 - \eta_s + \eta_c \eta_s} \tag{3}$$

Because both eqs 2 and 3 share the same denominator and the numerator in eq 3 is larger, the collection efficiency of this system is always better. Also, it will always be better than that of the single reverse-flow

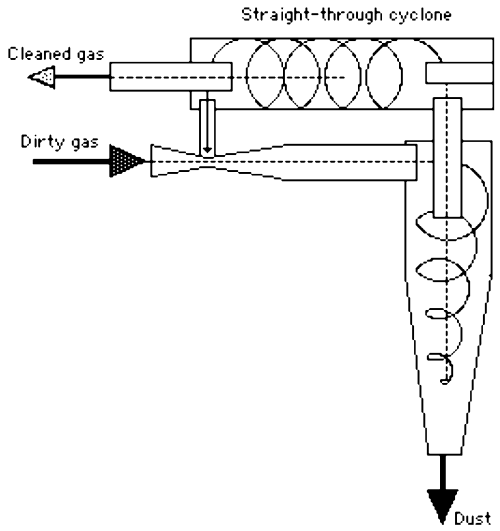

Figure 3. Proposed collector-first recirculation system.

cyclone operating within the loop, because the necessary condition $\eta_s(\eta_c - 1) < 0$ is always verified. To be fair, comparing the systems in Figures 2 and 3 makes sense only if they have similar geometries and sizes, which might not be the case because, in the proposed system (collector-first arrangement, Figure 3), the entire flow must pass through both the collector and concentrator, whereas in the system depicted in Figure 2 (concentrator-first arrangement), only the concentrator receives the entire flow, which might allow the collector, for comparable pressure losses, to be somewhat smaller and thus more efficient.

It was recently verified[26,39] that reverse-flow cyclones fitted with a post-cyclone (PoC) at the exit of the vortex finder can increase the collection of fines, but a significant reduction in emissions (about 33%) only occurs with a conical finned PoC at the expense of a large increase in pressure drop (about 1.2 kPa). However, when the bleed flow from the PoC is recycled back to the cyclone, significant collection improvements for submicrometer particle diameters occur with an increase of only 34% in the pressure drop above that of the cyclone. In this case, a reduction in emissions of about 26% has been reported.

In this work, the performance of a recirculation system with a collector-first arrangement is reported, with the collector being a single RS_VHE of 0.46-m inside diameter for the pilot-scale experiments and a set of 12 RS_VHEs of 0.50-m inside diameter in a parallel arrangement for the full-scale experiments. The pilot-scale concentrator has the same diameter as the pilot-scale RS_VHE cyclone (purely for convenience), whereas the two industrial-scale concentrators were larger to accommodate flow from six cyclones each, for a maximum increase in pressure drop of about 30% over that of the reverse-flow cyclones.

Experimental Section Results

Pilot-Scale Cyclones, Recirculation System, and Online Pulse Jet Bag Filter. At the laboratory scale, the 0.02-m-inside-diameter RS_VHE design showed, on average, a 53% reduction in emissions of fine $Ca(OH)_2$ (log-normal distribution, mean mass diameter of 1.37 μm, geometric standard deviation of 2.23) as compared to a similar-sized Stairmand HE design at comparable pressure losses.[6] When fitted with a collector-first recirculation system using a small venturi to promote recirculation (Figure 3), the emissions were further reduced by 57%, on average.[27] Thus, the recirculation system with the RS_VHE cyclone reduced emissions by almost 80% as compared to a single Stairmand HE design. A 50% reduction in emissions due to the recirculation has also been obtained at the laboratory scale with $CaCO_3$ (median mass diameter of 1.96 μm), again using an RS_VHE collector. These results were sufficiently encouraging to extend the RS_VHE and recirculation systems to pilot- and eventually to full-scale testing.

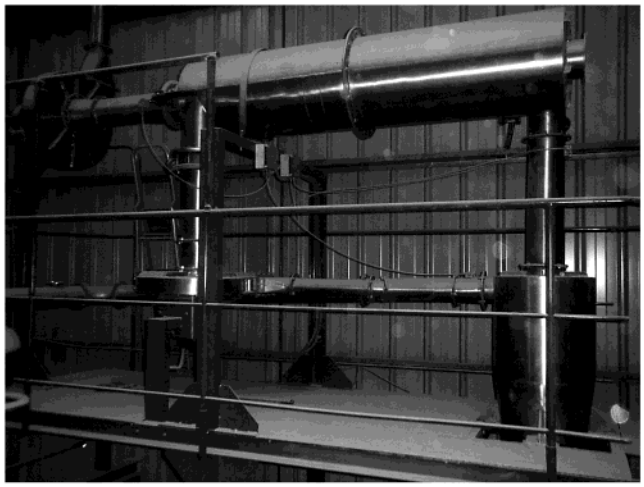

Figure 4. Pilot-scale system (RS_VHE cyclone and concentrator).

The pilot-scale test rig was installed at the sulfanilic acid production facility of a Portuguese manufacturer of benzene-derived organic chemicals. Basically, a fluidized-bed dryer conveys sulfanilic acid dust to a 0.80-m-diameter high-loadings process cyclone that returns a fraction to the dryer and conveys the finer fraction to a pulse jet bag filter at a flow rate of about 10 000 m^3/h, a moisture content of 4% (molar basis), a temperature of 350 K, and concentrations up to 20 g/m^3. By installing the pilot rig in parallel with the bag filter, a small fraction of the flow (about 10%) could be diverted by an induced fan to a single RS_VHE cyclone, fitted with an optional recirculation straight-through cyclone and corresponding induced recirculation fan. Both fans were equipped with variable-speed motors to allow the recirculation and main flow rates to be varied. Figure 4 shows the pilot-scale system, which was designed to handle up to 1000 m^3/h of process gas and 500 m^3/h of recirculation gas.

The sampling locations (inlet, outlet, and recirculation pipes) for the pilot-scale cyclones and for the filter were established, and the velocity was measured by complete pitot traverses using a Testo 400 unit. The measurements revealed fairly flat distributions at the inlet and outlet and a much more irregular distribution at the recirculation pipe, as can be seen in Figure 5a,b, because of constraints on the sampling location (directly upstream from the recirculation fan). Resampling with a pitot tube at the inlet and outlet for the same operating conditions showed consistent results (all within ±5%), but resampling at the recirculation pipe showed flow rates for the same operating conditions varying by as much as ±22%. Thus, data derived from these measurements (recirculation flow rate, concentrator collection efficiency, and particle size distributions of recirculated dust) should be viewed with caution.

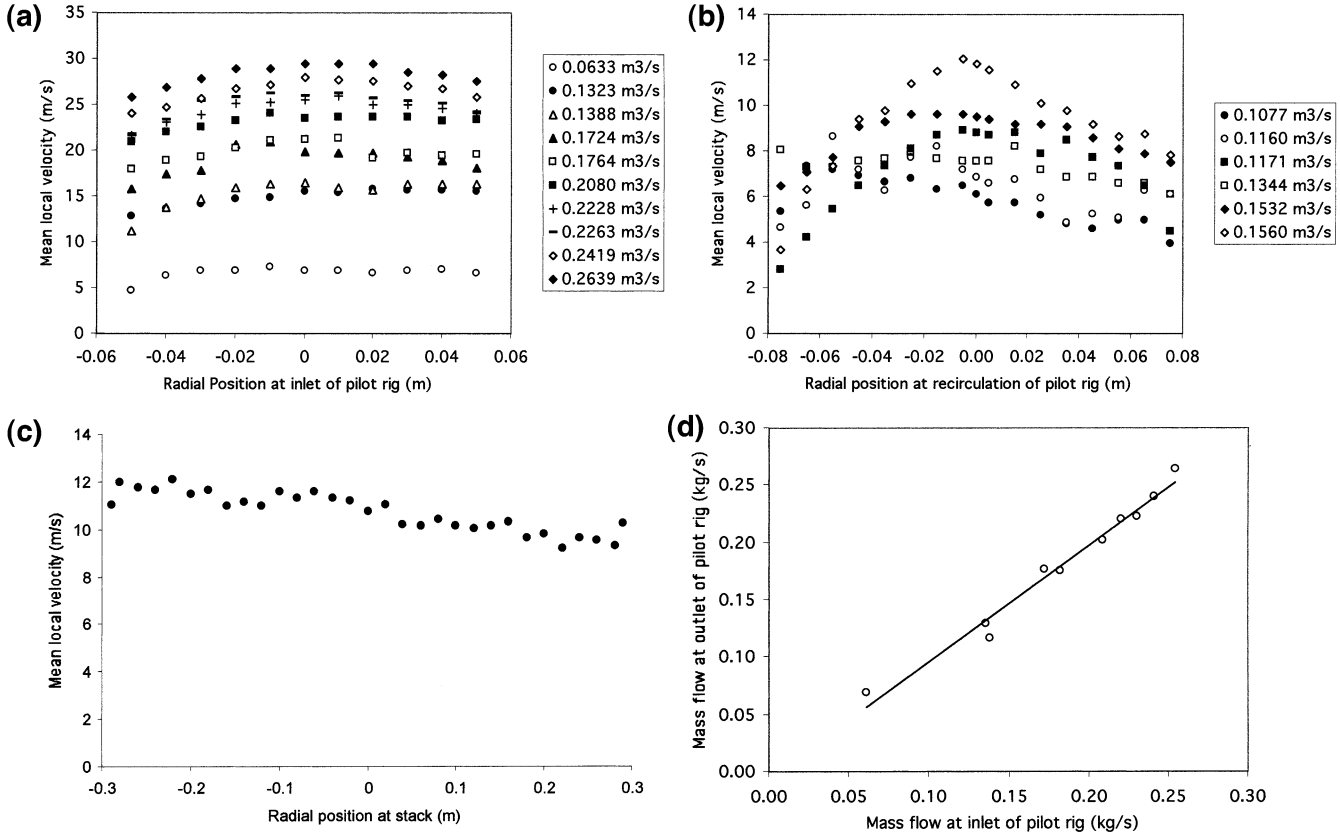

Figure 5. Velocity profiles: (a) inlet to pilot-scale cyclones, (b) recirculation to pilot-scale cyclones, and (c) stack. (d) Gas mass balances (pilot-scale).

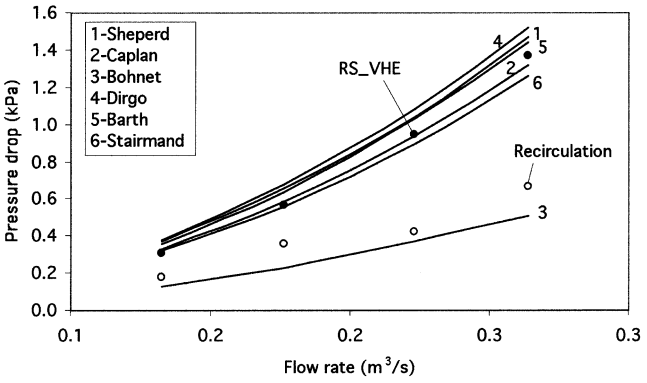

Figure 6. Pressure drop (pilot-scale RS_VHE and concentrator).

For the filter, the velocity profile was measured at the stack (Figure 5c) and was found to be somewhat skewed because of an inclined transition from the exhaust fan to the stack.

Although not shown, the velocity profiles at the outlet of the test cyclones are very similar to those at the inlet (Figure 5a). The agreement between the gas flow mass balances at the inlet and outlet of the test cyclones is excellent, as can be seen in Figure 5d.

To ascertain the accuracy of the measurements, the pilot-scale setup was temporarily disconnected, and the exhaust valve from the main induced draft fan was set completely open (97%). The computed gas flow rate from the pitot measurements (10 432 m^3/h) agrees well with the expected flow rate from the fan characteristic curve (about 11 000 m^3/h) at similar temperatures and total static pressures.

Figure 6 shows the pressure drop experienced by both the RS_VHE pilot-scale cyclone (collector) and the recirculation cyclone (concentrator) plotted against predictions (for the reverse-flow cyclone) by several models.[16,28−32] The model of Caplan[30] describes well the observed pressure drop, in contrast to the results for the laboratory-scale RS_VHE cyclone, where the model of Bohnet and Lorenz[32] gives much better predictions.[6] It is possible that different models are followed because of a size effect or because the laboratory-scale cyclone was made from polished machined aluminum whereas the pilot cyclone was made from welded stainless steel sheets. The pressure drop through the concentrator was much lower than that through the collector, typically by 50%.

Simultaneous sampling could not be performed because of the availability of a single Andersen M9096 stack sampler. To minimize errors due to process fluctuations, the pilot-scale station was fitted with SICK infrared optical sensors (FWM56 for the sender/receiver unit, FWR56 for the reflector unit, and FWA56-I for the evaluation unit). Whenever the production process was not stable, the instability could be immediately detected from the output of these sensors, at which point experimental sampling was terminated, and the corresponding data were discarded.

The sulfanilic acid that escapes from the process cyclone and enters the test cyclone is very fine (median volume diameter of about 17 μm with 6 wt % < 1 μm), as shown in Figure 7. This figure also shows the inlet distribution to the bag filter, computed from the bag filter catch and from sampling performed isokinetically at the stack with the Andersen sampler. The particle size distributions were measured with a Coulter LS230 laser sizer, and it can be concluded that the input distributions to the pilot-scale cyclones and the bag filter are similar. Also, the particle size distributions at the

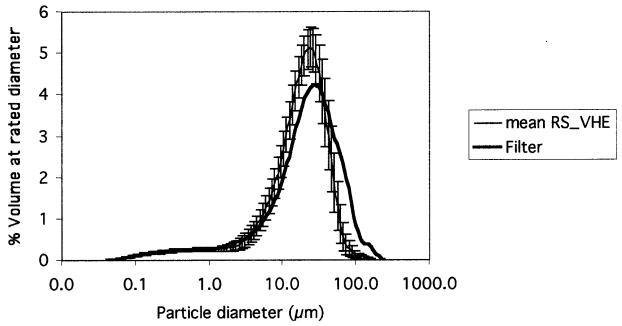

Figure 7. Inlet distribution to the pilot-scale cyclones and bag filter.

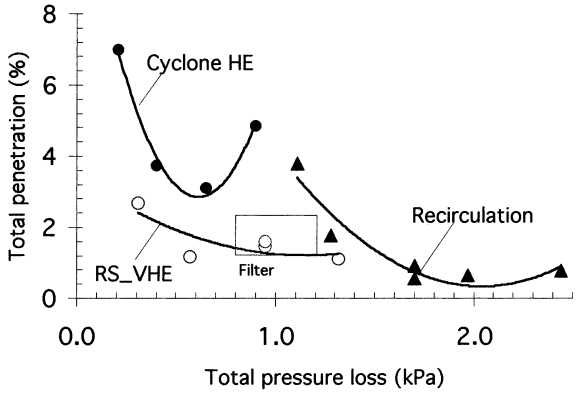

Figure 8. Global collection (pilot-scale cyclones and filter).

inlet are all similar, with an average standard error on the distributed volume of 16.4%.

Table 1 shows the experimental global collection, inlet, and outlet loads and operating conditions for all runs performed with the pilot-scale cyclones and the bag filter. Figure 8 shows the global penetrations as a function of the total pressure drop. It is more instructive to show penetrations (100% − percent collection efficiency) rather than collection efficiency, as this amplifies relative differences for high collection efficiencies. For example, two dedusters having collection efficiencies of 98 and 99% show a large relative difference in penetration (50%) but a marginal relative difference in collection (about 1%) for the same absolute difference in collection or penetration (1%).

A comparison was also made with the performance of a competing high-efficiency (HE) cyclone available on the marketplace (inside diameter $D = 0.33$ m, $a/D = 0.64$, $b/D = 0.28$, $s/D = 0.50$, $D_e/D = 0.58$, $h/D = 1.75$, $D_b/D = 0.40$, $H/D = 3.66$) and with the bag filter. The pressure drop across the bag filter was not measured, and the results in Figure 8 reflect the range given by the filter maker (0.8−1.2 kPa). However, because the compressed air was set to be activated on-demand in the differential range of 1.5−1.8 kPa, the actual pressure drop must be higher. The RS_VHE cyclone shows collection efficiencies comparable to those of the bag filter (which showed two measured efficiencies of 97.78 and 98.65%), and significantly better than those of the HE cyclone (which showed a maximum measured efficiency of 96.90% and severe dust reentrainment, as will be seen below). However, in the case of recirculation, the RS_VHE system actually performed better than the bag filter, showing a reduction in emissions of up to 58%, corresponding to a collection of 99.44%, albeit at the expense of a somewhat larger pressure drop.

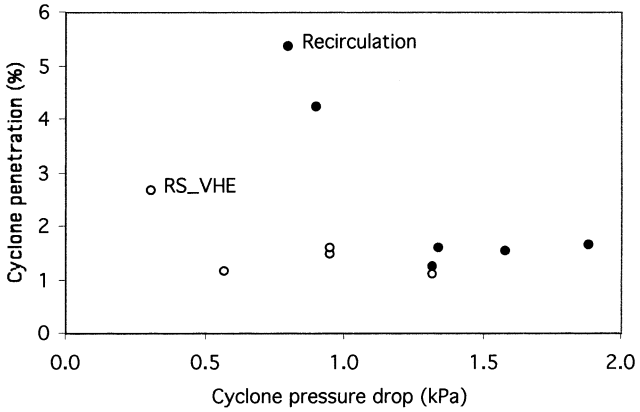

Figure 9. Cyclone in-loop penetration.

Table 1 shows that the recirculation efficiency η_s, measured by isokinetic sampling, except for the lower recirculation fraction, is roughly independent of the fraction of gas recirculated, with an average value of 50%. Table 1 also shows the cyclone efficiency within the loop, computed from eq 3. However, because of the unstable velocity profiles obtained at the recirculation sampling station (Figure 5b), these results should be considered only as approximations. Figure 9 shows that the cyclone inloop penetration (100% − percent cyclone collection from eq 3) increases in the presence of recirculation if the cyclone pressure drop is small.

Table 1. Experimental Data (Pilot-Scale Cyclones and Filter)

device	run	total flow (m^3/s)	velocity (m/s)	cyclone ΔP (kPa)	total ΔP (kPa)	load (mg/m^3)	emissions (mg/m^3)	collection η (%)	cyclone η_c[a] (%)	recirculation fraction (%)	recirculation η_s (%)
pilot RS_VHE	1	0.2639	18.03	1.32	1.90	7760	81	98.91	–	–	–
	2	0.2228	15.23	0.95	1.29	7714	117	98.41−98.53	–	–	–
	3	0.1764	12.05	0.57	0.93	5886	79	98.84	–	–	–
	4	0.1323	9.04	0.31	0.45	3288	90	97.32	–	–	–
pilot recirculation	5	0.2132	14.57	1.32	1.70	8484	44	99.44	98.76	73.2	55.3
	6	0.2575	17.60	1.58	1.97	5350	36	99.35	98.46	45.5	58.3
	7	0.3730	25.49	1.88	2.44	5097	40	99.22	98.34	41.0	53.4
	8	0.3059	20.91	1.34	1.70	4286	43	99.08	98.42	43.9	42.3
	9	0.3430	23.44	0.90	1.28	5544	98	98.22	95.77	31.4	59.0
	10	0.3622	24.75	0.80	1.11	8809	337	96.20	94.64	32.0	30.2
cyclone HE	11	0.2639	13.67	0.90	1.65	8761	414	95.15	–	–	–
	12	0.2228	11.54	0.65	1.15	8860	272	96.90	–	–	–
	13	0.1764	9.14	0.40	0.76	5395	418	96.27	–	–	–
	14	0.1323	6.90	0.21	0.42	7288	300	93.01	–	–	–
filter	15	3.023	–	–	0.8−1.2	9870	219	97.87	–	–	–
	16	3.023	–	–	0.8−1.2	15 400	207	98.65	–	–	–

[a] Calculated using eq 3.

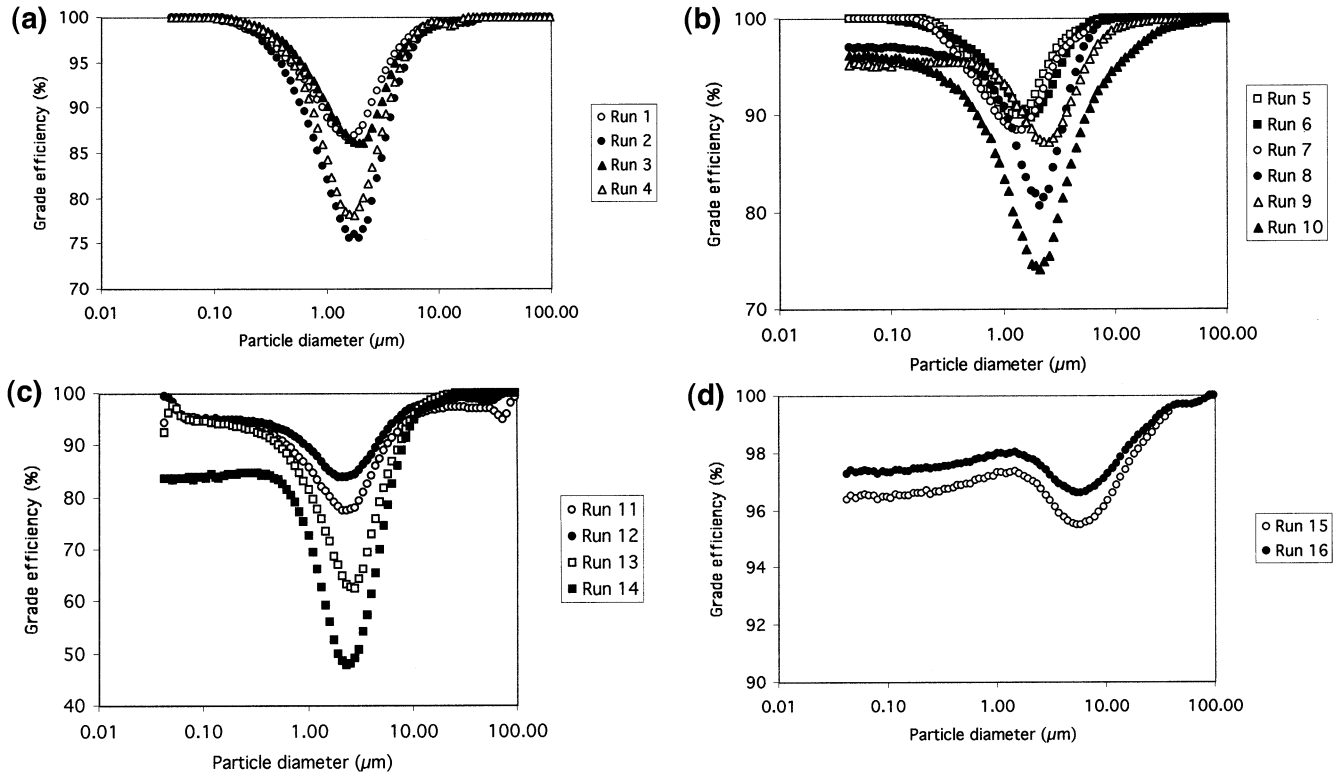

Figure 10. Grade efficiencies of (a) the pilot-scale RS_VHE cyclone, (b) the recirculation system, (c) the pilot-scale HE cyclone, and (d) the pulse jet bag filter.

Because the recirculation reinjects finer particles at the cyclone inlet, its in-loop efficiency should, in principle, decrease, and this becomes important for low cyclone pressure drops (below about 1 kPa), viz., for low cyclone collection efficiencies. Figure 9 shows that the cyclone penetration remains essencially constant at about 1.3% for cyclone pressure drops above about 1 kPa, indicating a large range of inlet velocities for maximum cyclone collection (15−25 m/s). This suggests that, with recirculation, it is not the cyclone inlet velocity that matters, but rather the cyclone pressure drop.

Figure 10a−d shows the grade efficiencies of the pilot-scale cyclones and the bag filter computed from the global efficiencies and the particle size distributions of the corresponding experiments as measured by a Coulter LS 230 laser sizer.

Figure 10a shows the results obtained with the pilot-scale RS_VHE cyclone in the absence of recirculation at varying gas flow rates. Two experiments were performed at the same average velocity (and pressure drop), showing good agreement in the global collection (98.41−98.53%). The results suggest that increasing the cyclone average inlet velocity from 9 m/s (run 4) to 18 m/s (run 1) increases collection from about 97.3 to 98.9%. However, in the intermediate range, the data show an unexpected behavior, with a lower velocity of 12 m/s (run 3) corresponding to a higher collection (98.8%) than a higher velocity of 15 m/s (run 2, 98.5%). However, the difference is small and might be within the experimental error. From the data, we can conclude that, between 12 and 18 m/s, the pilot-scale RS_VHE cyclone has an efficiency of 98.7 ± 0.4%, roughly independent of the inlet velocity.

Figure 10b shows the results obtained with the pilot-scale RS_VHE cyclone in the presence of recirculation at varying gas flow rates. Low efficiencies (<99%) are obtained for low cyclone pressure drops (<1 kPa, runs 9 and 10), and high efficiencies, corresponding to high cyclone in-loop efficiencies (Table 1), are obtained for higher cyclone pressure drops (>1.3 kPa, runs 5−8). The highest efficiency (99.44%) was obtained with the highest recirculation fraction (73.2%, run 5).

Figure 10c shows the results obtained with the HE cyclone in the absence of recirculation at varying gas flow rates. Comparing plots a and c of Figure 10 shows that the HE cyclone has a lower collection for larger particles at high velocities, possibly as a result of particle reentraiment, which occurs in the HE cyclone with velocities as low as 11.5 m/s and is very severe at velocities of 13.7 m/s. Such reentraiment does not occur with the RS_VHE cyclone for velocities as high as 18 m/s.

Figure 10d shows that the bag filter captures dust with essentially the same degree for a large range of particle sizes, as expected.[33] Because only one particle size distribution was measured at the filter outlet (run 16, Table 1), the grade efficiency curves for the other runs are only estimates. The filter was designed on the basis of unavailable data (dust load and particle size distribution) with an actual air-to-cloth ratio of 30 s/m (64 polyester 500 g/m^2 bags, 152 × 3000 mm, total collecting area of 92 m^2). Because the actual particle size distribution is about 1 order of magnitude smaller than expected at the design and commissioning stages of the bag filter, viz., median size of about 20 versus 250 μm, the fluidized dryer conveys much finer particles that escape the process cyclone at much increased loads. This explains the very short periods between filter shut down for bag cleaning and/or replacement (every 6 months).

Although not done here, it can be shown that, above about 2 μm, there is good agreement between the grade efficiency curves predicted using the Mothes and Loffler[7] model coupled with eq 1 and the experimental data, both

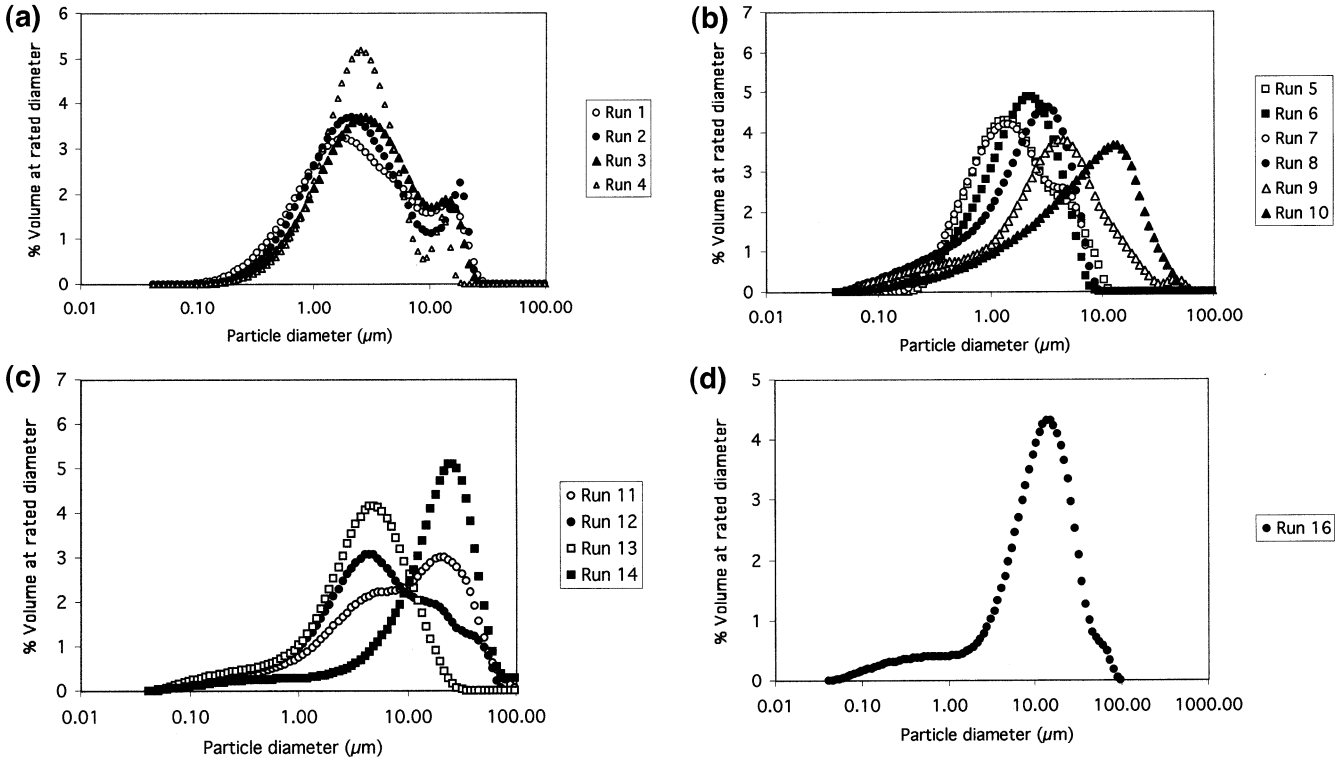

Figure 11. Outlet distributions from (a) the pilot-scale RS_VHE cyclone, (b) the recirculation system, (c) the pilot-scale HE cyclone, and (d) the pulse jet bag filter.

for the RS_VHE and HE cyclones and for the recirculation system. The Mothes and Loffler[7] model had to be adapted for modeling of the recirculation system, as will be discussed in another paper. It can be seen that all grade efficiency curves for the cyclones exhibit a minimum in collection efficiency and that particles smaller than about 2 μm are collected with much larger efficiencies than expected.

The unexpectedly high collection of fine particles in cyclones has been observed before with small laboratory-scale Stairmand HE sampling cyclones with inside diameters of 0.023−0.07 m collecting fly ash at loadings of 50−0.8 g/m^3, with tails shifting from 3 to 1.5 μm as the loading decreases.[34] The loadings for the pilot-scale cyclones varied from 3.3 to 8.9 g/m^3, and agglomeration might be one possible explanation for this high collection, because the agglomerates were collected as larger particles and subsequently measured by the laser sizer as individual particles. Bernard et al.[35] also found tails in the grade efficiency curves starting at about 2 μm. Hoffmann et al.[36] observed the same phenomenon with 0.2-m Stairmand HE cyclones at loadings of 5.3 g/m^3, but because this occurred below 0.8 μm, capture of small particles by large ones by Brownian diffusion could be the cause. Zhao et al.[26] also reported the occurrence of "duck tails" between 0.45 and 0.9 μm, which they attributed to fine particle agglomeration in their high-efficiency (PoC-fitted) cyclones. Recent (unpublished) work performed by one of the authors at the laboratory scale with 0.02-m RS_VHE cyclones and fine $CaCO_3$ at loadings of 1−2 g/m^3 also showed tailings starting at about 0.8 μm. It is possible that the above phenomena are present to some degree, leading to the observed higher collection of the finer fraction. However, if the fine dust enters the cyclone agglomerated, then it should also enter the bag filter agglomerated, in which case the fine fraction should have also been captured in this device with close to 100% efficiency. Because this did not occur, the data presented here suggest that the capture of small particles by large ones in the turbulent cyclone flow field is the main cause of the observed extremely high collection efficiencies.

Still another possible cause is particle−particle interactions at high loadings (above 10 g/m^3), where fine particles are displaced to the underflow as a result of blockage of their movement toward the inner vortex by larger particles.[37,38] Because these duck tails also occur at low loadings, however, this is perhaps the least likely explanation. Nevertheless, it is clear that further studies are needed to clarify this phenomenon.

Figure 11a−d shows the outlet particle size distributions of the pilot-scale cyclones and bag filter. The difference between the distributions of the single RS_VHE and HE cyclones is already remarkable, but the recirculation system removes all particles larger than about 8−10 μm. The distribution at the outlet of the bag filter is completely different from that of the cyclones, showing both more smaller and more larger particles, and is similar (except for the larger particles that are absent from the outlet) to the inlet size distribution (Figure 7).

The particle size distributions (not shown) of the recirculated dust are similar to the outlet distributions from the system (Figure 11b). This behavior is similar to that observed by Zhao et al.[26] in the recirculated bleed from the PoC-fitted cyclones.

Industrial-Scale Cyclones. Based on the pilot-scale results, a system of 12 RS_VHE cyclones (0.5-m inside diameter) and 2 recirculation cyclones was built for the recovery of sulfanilic acid from a 14 000 m^3/h gaseous stream exiting the process cyclone located at the outlet of the fluidized-bed dryer. This system was used to replace the pulse jet bag filter, as it operates with a higher collection efficiency, comparable operating costs,

Figure 12. Industrial-scale RS_VHE and recirculation cyclones.

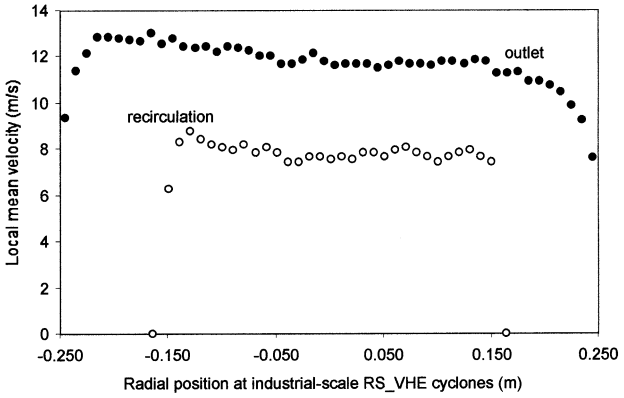

Figure 13. Velocity traverse at the outlet of the industrial-scale RS_VHE and recirculation cyclones.

and expected lower maintenance costs. Figure 12 shows the RS_VHE and recirculation cyclones already in operation at the sulfanilic acid production facility.

Figure 13 shows velocity traverses performed at the exhaust and recirculation pipes of the system for the maximum recirculation compatible with the process fan (about 21%, because it does not have a variable-speed motor and some negative pressure is needed at the fluidized dryer). Similar profiles were obtained for different recirculation fractions and were used to establish the necessary conditions for isokinetic sampling (outlet) and for flow calculations (outlet and recirculation). At the present moment, the maximum flow rate without recirculation was measured to be 10 432 m^3/h, which is well below the 14 000 m^3/h specified at the design stage. Because recirculation decreases the outlet flow, four cyclones were temporarily taken out of service. This allowed the pressure drop through the cyclones (with recirculation) to be around 1.9 kPa, which is in the optimum operating range according to the pilot-scale experiments (see Figure 9).

Table 2 shows the results of these isokinetic samplings and the measured overall collection efficiencies. Because it was not possible to establish adequate sampling locations at the cyclones' inlets, the inlet

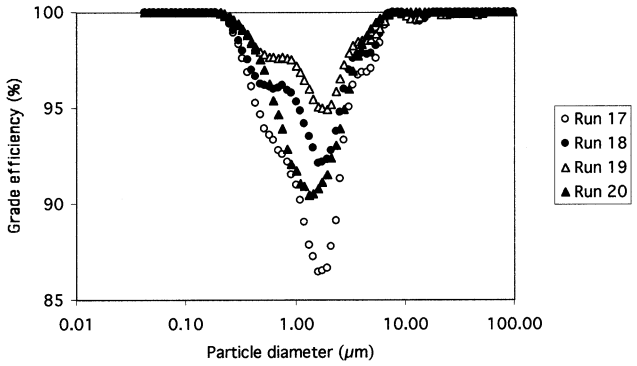

Figure 14. Grade efficiencies (industrial recirculation system).

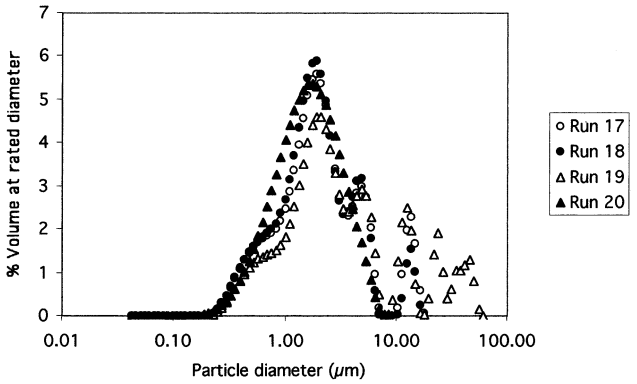

Figure 15. Size distributions (industrial recirculation system).

distribution was computed from the catch and outlet distributions and mass flows. In this way, simultaneous sampling could, in fact, be approached, as the cyclones' catches throughout outlet sampling were directed to a bag for subsequent weighing.

Figure 14 shows the grade efficiencies obtained. Clearly, the full-scale cyclones are behaving much like the pilot-scale ones, especially for a recirculation of 21%. This is not surprising because they are of similar size. By comparison with Figure 10d, the bag filter exhibits higher collection than the cyclones only over a small particle size range (0.4−3.7 μm).

Figure 15 shows the particle size distributions obtained at the inlet and outlet for the full-scale cyclones. The recirculation system has removed essentially all particles above 8 μm for 21% recirculation. With lower recirculations, this removal was not as efficient, and particles above 10 μm were present in the emissions.

Conclusions

This paper presents experimental data collected for both pilot- and full-scale numerically optimized RS_VHE cyclones. Previous laboratory results with a small 0.02-m RS_VHE cyclone capturing $Ca(OH)_2$ and $CaCO_3$ showed its superiority over the Stairmand HE design.[5,6] These results have been extended to pilot and industrial scale with 0.46−0.50-m-diameter RS_VHE cyclones and a coupled recirculation system, in a collector-first ar-

Table 2. Results Obtained in Full-Scale Tests

run	actual load (g/m^3)	total flow rate (m^3/s)	catch (kg/h)	total ΔP (kPa)	cyclone ΔP (kPa)	efficiency (%)	emissions (mg/m^3)	recirculation (%)
17	10.04	2.891	90.8	2.61	1.97	99.21	80	12.4
18	10.98	3.078	99.7	2.52	1.90	99.58	46	12.3
19	15.60	2.912	141.7	2.60	1.95	99.64	56	13.0
20	7.73	2.819	61.5	2.40	1.90	99.60	31	21.3

rangement, capturing fine sulfanilic acid (17-μm median volume diameter) at a Portuguese chemical manufacturer. The RS_VHE cyclones are significantly more efficient than a high-efficiency cyclone available on the marketplace, and the coupled recirculation system is significantly more efficient than the tested pulse jet bag filter.

With partial recirculation, the emissions were about 75% lower than those from competing high-efficiency cyclones, and collection efficiencies of 99.6% were achieved at inlet concentrations of about 8 g/m^3 and a recirculation fraction of about 21%. The results obtained at the laboratory, pilot, and industrial scales suggest that the numerically optimized reverse-flow cyclones, when coupled with a partial recirculation system, can be used to meet emission standards and fine product recovery as an alternative to on-line pulse jet bag filters or venturis.

Acknowledgment

The authors thank the Portuguese Innovation Agency through Contract P0060/IC-PME/I/II/M-RS_VHE. We also thank our collaborators Andreia Pereira (FEUP, Prodep III grant) and Maria Dolores (Universidad de Valladolid, Erasmus grant) for help with the pilot-scale experiments.

Notation

a = height of tangential entry (m)
b = width of tangential entry (m)
D = cyclone diameter (m)
D_b = cyclone dust discharge diameter (m)
D_e = vortex finder diameter (m)
d_p = particle diameter (m)
D_r = dispersion coefficient (m^2 s^{-1})
h = height of cylindrical body (m)
H = total cyclone height (m)
Pe_p = radial particle Peclet number
Re_p = radial particle Reynolds number
s = vortex finder length (m)
u_r = particle radial velocity (m s^{-1})

Greek Letters

μ = gas viscosity (kg m^{-1} s^{-1})
ΔP = pressure loss (Pa)
η_c = cyclone collection efficiency
η_s = concentrator collection efficiency
ρ = gas density (kg m^{-3})

Acronyms

HE = high efficiency
VHE = very high efficiency

Literature Cited

(1) Zenz, F. A. Cyclone design tips. *Chem. Eng.* **2001**, *108* (1), 60.

(2) Licht, W. *Air Pollution Control Engineering—Basic Calculations for Particulate Collections*; Marcel Dekker: New York, 1980.

(3) Berezowski, M.; Warmuzinski, K. Gas recycling as a means of controlling the operation of cyclones. *Chem. Eng. Process.* **1993**, *32*, 345.

(4) Ogawa, A. Mechanical Separation Process and Flow Patterns of Cyclone Dust Collectors. *Appl. Mech. Rev.* **1997**, *50* (3), 97.

(5) Salcedo, R. L.; Coelho, M. A. Turbulent Dispersion Coefficients in Cyclone Flow—An Empirical Approach. *Can. J. Chem. Eng.* **1999**, *77* (Aug), 609.

(6) Salcedo, R. L.; Cândido, M. G. Global optimization of reverse-flow gas cyclones: Application to small-scale cyclone design. *Sep. Sci. Technol.* **2001**, *36* (12), 2707.

(7) Mothes, H.; Loffler, F. Prediction of particle removal in cyclone separators. *Int. Chem. Eng.***1988**, *28*, 231.

(8) Iozia, D. L.; Leith, D. The logistic function and cyclone fractional efficiency. *Aerosol Sci. Technol.* **1989**, *12*, 598.

(9) Clift, R.; Ghadiri, M.; Hoffman, A. C. A critique of two models for cyclone performance. *AIChE J.* **1991**, *37*, 285.

(10) Salcedo, R. L.; Fonseca, A. M. Grade efficiencies and particle size distributions from sampling cyclones. In *Mixed-Flow Hydrodynamics*; Cheremisinoff, P., Ed.; Gulf Publishers: Houston, TX, 1996; Chapter 23, p 539.

(11) Hoffmann, A. C.; van Santen, A.; Allen, R. W. K. Effects of geometry and solid loading on the performance of gas cyclones. *Powder Technol.* **1992**, *70*, 83.

(12) Li, Z.; Zisheng, Z.; Kuotsung, Yu. Study of structure parameters of cyclones. *Chem. Eng. Res. Des.* **1988**, *66* (Mar), 114.

(13) Schmidt, P. Unconventional cyclone separators. *Int. Chem. Eng.* **1993**, *33* (1), 8.

(14) Lidén, G.; Gudmundsson, A. Semi-empirical modeling to generalise the dependence of cyclone collection efficiency on operating conditions and cyclone design. *J. Aerosol Sci.* **1997**, *28* (5), 853.

(15) Dirgo, J.; Leith, D. Performance of theoretically optimized cyclones. *Filtr. Sep.* **1985**, *22*, 119.

(16) Iozia, D. L.; Leith, D. Cyclone optimization. *Filtr. Sep.* **1989**, *26* (Jul—Aug), 272.

(17) Ramachandran, G.; Leith, D. Cyclone Optimization Based on a New Empirical Model for Pressure Drop. *Aerosol Sci. Technol.* **1990**, *15*, 135.

(18) Salcedo, R. L.; Campos, J. A. G. Optimization for Pollution Reduction: A Numerical Approach to Cyclone Design. In *Proceedings of the 2nd Conference on Process Integration, Modeling and Optimization for Energy Saving and Pollution Reduction*; 1999, p 57.

(19) Ravi, G.; Gupta, S.; Ray, M. B. Multiobjective optimization of cyclone separators using genetic algorithm. *Ind. Eng. Chem. Res.* **2000**, *39*, 4272.

(20) Leith, D.; Licht, W. The collection efficiency of cyclone type particle collectors—A new theoretical approach. *AIChE Symp. Ser.* **1972**, *126*, 196—206.

(21) Salcedo, R. L. Solving Non-Convex NLP and MINLP Problems with Adaptive Random Search. *Ind. Eng. Chem. Res.* **1992**, *31* (1), 262.

(22) Moore, M. E.; McFarland, A. R. Performance Modeling of Single-Inlet Aerosol Sampling Cyclones. *Environ. Sci. Technol.* **1993**, *27*, 1842.

(23) Moore, M. E.; McFarland, A. R. Design Methodology for Multiple Inlet Cyclones. *Environ. Sci. Technol.* **1996**, *30*, 271.

(24) Crawford, M. *Air Pollution Control Theory*; McGraw-Hill: New York, 1976; p 152.

(25) Wysk, R.; Smolensky, L. A. Novel particulate control device for industrial cleaning. *Filtr. Sep* **1993**, *30* (Jan—Feb), 29.

(26) Zhao, W. A. S.; Mujundar Ray, M. B. Collection efficiencies of various designs of post cyclone. *Can. J. Chem. Eng.* **2001**, *79*, October, 708.

(27) Cândido, M. G. Recirculation cyclones for fine particle collection. M.Eng. Thesis in Environmental Engineering, Faculdade de Engenharia da Universidade do Porto, Porto, Portugal, 2000 (in Portuguese).

(28) Shepherd, C. B.; Lapple, C. E. Flow pattern and pressure drop in cyclone dust collectors. *Ind. Eng. Chem.* **1939**, *31*, 979.

(29) Barth, W. Design and layout of the cyclone separator on the basis of new investigations. *Brenst.—Warme—Kraft* **1956**, *8*, 1.

(30) Caplan, K. J. Source control by centrifugal source and gravity. In *Air Pollution*; Stern, A. C., Ed.; Academic Press: New York, 1968; Volume 3, Chapter 43, p 366.

(31) Dirgo, J. Relationships between cyclone dimensions and performance. Ph.D. Thesis, Harvard University, Cambridge, MA, 1988.

(32) Bohnet, M.; Lorenz, T. Separation efficiency and pressure drop of cyclones at high temperatures. In *Gas Cleaning at High Temperatures*; Clift, R., Seville, J. P. K., Eds.; Blackie Academic and Professional: London, 1993; pp 17—31.

(33) Croom, M. L. *Filter Dust Collectors—Design and Application*; McGraw-Hill: New York, 1994.

(34) Salcedo, R. L. R. Collection Efficiencies and Particle Size Distributions from Sampling Cyclones−Comparison of Recent Theories with Experimental Data. *Can. J. Chem. Eng.* **1993**, *71*, 20.

(35) Bernard, J. G.; Andries, J.; Scarlett, B. Cyclone performance at various temperatures. In *Proceedings of Filtech Europa 91*; Taylor, M. J., Ed.; The Filtration Soiety: London, 1991; pp 591−599.

(36) Hoffmann, A. C.; de Groot, M.; Hospers, A. The effect of the dust collection system on the flowpattern and separation efficiency of a gas cyclone. *Can. J. Chem. Eng.* **1996**, *74*, 464.

(37) Stairmand, C. J. The Design and Performance of Cyclone Separators. *Trans. Inst. Chem. Eng.* **1951**, *9*, 356.

(38) Hsieh, K. T.; Rajamani, R. K. Mathematical Model of the Hydrocyclone Based on Physics of Fluid Flow. *AIChE J.* **1991**, *7*, 735.

(39) Ray, M. B.; Luning, P. E.; Hoffmann, A.; Plomp, A.; Beumer, M. I. L. Post cyclone (PoC): An innovative way to reduce the emission of fines from industrial cyclones. *Ind. Eng. Chem. Res.* **1997**, *36*, 2766.

Received for review March 13, 2002
Revised manuscript received October 10, 2002
Accepted October 18, 2002

IE020195E